J Seismol (2020) 24:37–53
https://doi.org/10.1007/s10950-019-09883-6

ORIGINAL ARTICLE

Check for updates

Recent seismicity in northern European Russia

Alexey N. Morozov · Natalya V. Vaganova · Yana V. Konechnaya · Irina A. Zueva · Vladimir E. Asming · Nataliya N. Noskova · Nikolay V. Sharov · Bela A. Assinovskaya · Natalyia M. Panas · Zinaida A. Evtyugina

Received: 19 May 2019 / Accepted: 26 September 2019 / Published online: 4 December 2019

Abstract A revised comprehensive catalog has been made for earthquakes that occurred in northern European Russia for the period between 2005 and 2017. The earthquake parameters were determined to greater accuracy using the same velocity model (BARENTS), the same location method (based on generalized beamforming), combining data from catalogs, bulletins, and (in part) from waveform supplied by regional seismograph networks in Russia and the Scandinavian countries. The resulting unified catalog formed a basis to assess the recent seismicity in northern European Russia, which occurs as low magnitude earthquakes. The distribution of earthquake epicenters is not uniform. The Fennoscandian Shield shows the highest activity (by seismicity rate and epicenter density), the next to follow are the northeastern Russian plate and the northern Urals Fold-Thrust Region. All earthquakes typically occurred at crustal depths.

Keywords Northern European Russia · Earthquake · East European Platform · Fennoscandian Shield · Urals · Revised Earthquake catalog · Recent seismicity

A. N. Morozov · B. A. Assinovskaya · N. M. Panas
Geophysical Survey of Russian Academy of Sciences, Lenina av. 189, Obninsk, Kaluga region, Russia 249035

A. N. Morozov (✉) · N. V. Vaganova · Y. V. Konechnaya
Department of Seismology, N. Laverov Federal Center for Integrated Arctic Research, Severnoj Dviny St., 23, Arkhangelsk, Russia 163000
e-mail: morozovalexey@yandex.ru

N. V. Vaganova
e-mail: nvag@yandex.ru

Y. V. Konechnaya
Sector of seismic monitoring of the north of the Russian plate, Geophysical Survey of Russian Academy of Sciences, Severnoj Dviny St., 23, Arkhangelsk, Russia 163000

I. A. Zueva · N. V. Sharov
Institute of Geology of the Karelian Research Centre of the Russian Academy of Sciences, Pushkinskaya St., 11, Petrozavodsk, Karelia, Russia 185910

I. A. Zueva
e-mail: ek92wa@mail.ru

V. E. Asming · Z. A. Evtyugina
Kola Branch of Geophysical Survey of Russian Academy of Sciences, Fersmana St., 14, Apatity, Russia 184209

V. E. Asming
e-mail: asmingve@mail.ru

N. N. Noskova
Institute of Geology of the Komi Science Center of the Ural Branch of the Russian Academy of Sciences, Pervomaiskaya Str., 54, GSP-2, Syktyvkar, Komi Republic, Russia 167982
e-mail: nataliyageo@mail.ru

1 Introduction

The area of study is delineated in Fig. 1; it comprises (from west to east) the northern East European Platform (EEP), the Pechora plate, and the northern Ural Fold-Thrust Region that bound the latter plate from the east. In tectonic terms, most of northern European Russia consists of parts of the EEP, namely, the Russian plate and the Fennoscandian Shield.

The East European Platform (EEP) is a feature whose level of seismic activity is rather low. For this reason, the EEP has for a long time not been a priority for seismic monitoring carried out in the USSR, and later on in the Russian Federation, because platform areas were commonly thought to be aseismic (Malovichko et al. 2007). However, the high level of urbanization, the presence of critical and ecologically hazardous facilities, major industrial centers, an intensive development of nuclear, chemical, and mining industries all tended to draw attention to the need for a more careful study of any seismic processes in platform areas (Starovoit 2005; Adushkin 2016).

Since the mid-1990s, regional seismic networks began to be developed in the EEP area with an active assistance on the part of the Geophysical Survey of the Russian Academy of Sciences (GS RAS). The networks were intended to conduct instrumental observation of tectonic, man-induced, and geo-ecologic processes as they were evolving over time (Malovichko et al. 2007). Researchers could now assess the manifestations of recent seismicity in the platform and to use these data for subsequent geological, tectonic, and geodynamic inferences, as well as for more reliable determination of seismicity levels in various regions (Yudakhin et al. 2003; Shchukin 2007; Adushkin 2013).

The regional seismic networks began to be developed at the highest rate in northern European

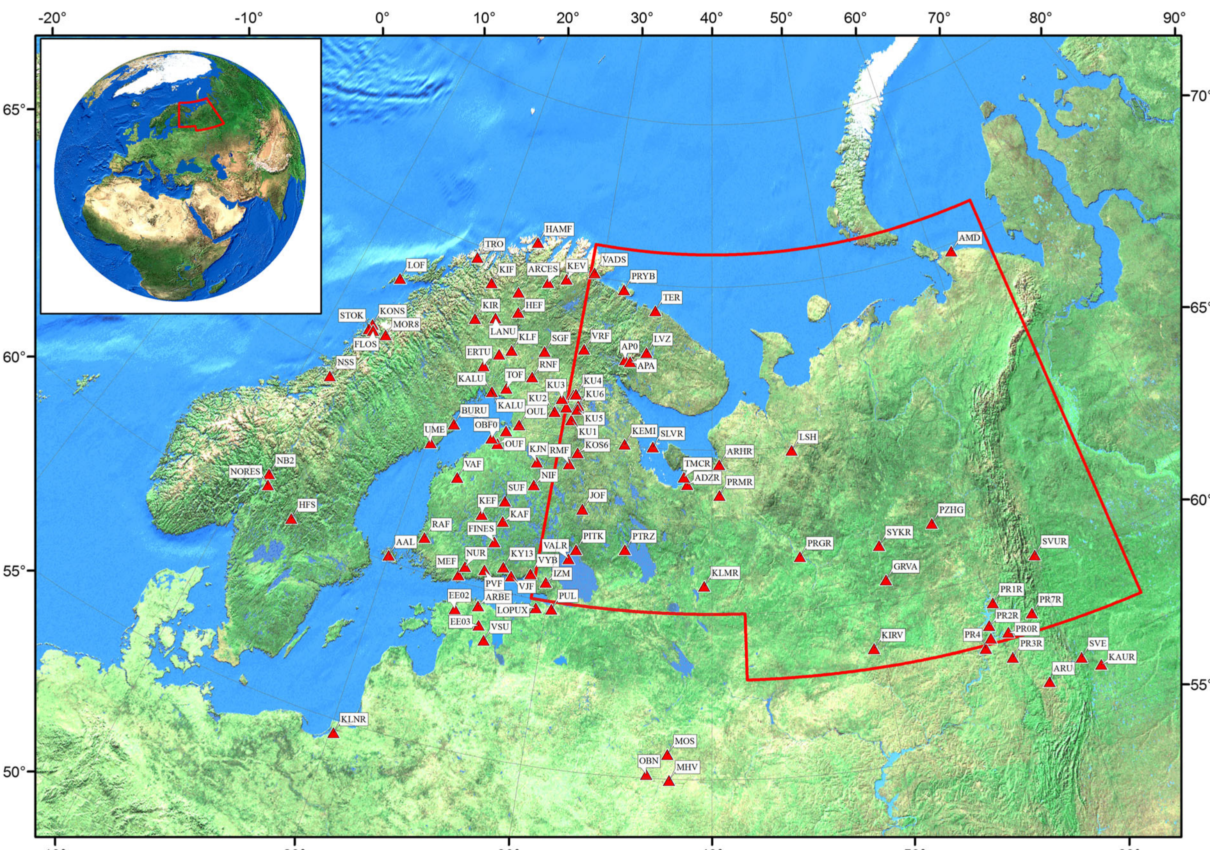

Fig. 1 The seismic stations whose data were used to develop a revised comprehensive earthquake catalog for northern European Russia. The line delineates the area of study

Russia: in Leningrad, Arkhangelsk, and Murmansk Regions, in the republics of Karelia and Komi. As a result, since 2004 northern European Russia had the highest density of seismometric observation for the entire instrumental period of observation (Fig. 1). This ensured a wide range of epicentral distance and a greater azimuthal coverage of recorded seismic events.

The expansion of the seismological network became an important event for Russian seismology, because some historical and, later on, economic factors, prevented the organization of systematic and purposeful observations of seismic processes (Nikonov 2013). A single seismic station was operated during the instrumental period between 1907 and 1956 (Pulkovo, PUL). It was only during the preparation for the International Geophysical Year of 1957–58 (Collis, C., and Dodds 2008) that the Apatity seismic station was installed in northwestern European Russia in 1956 (Fig. 1). However, these stations could not record even moderate seismic events, let alone small ones. The factors responsible for this state of affairs include a high level of seismic noise at Pulkovo and the remoteness of the Apatity station. Three more seismic stations were added to Apatity in the 1970s, and this made it possible to reliably record small earthquakes in northwestern European Russia (Vinogradov et al. 2016).

However, the regional seismic networks available in northern European Russia were set up and operated independently of each other. As a result, the earthquake parameters were different at different seismological centers, because the determinations were mostly based on their own observations only. We therefore combined the work of seismologists affiliated to the regional seismic networks in northern European Russia in order to combine the respective catalogs, bulletins, and, in part, waveform. This resulted in combined bulletins for the earthquakes that have been recorded in northern European Russia during the period from 2005 to 2017; these bulletins were then used for hypocenter relocation based on the same velocity model and the same location procedure. The present paper aims at developing a revised comprehensive catalog that can be used for assessment of recent seismicity in northern European Russia.

2 A description of seismicity and instrumental observations

The main sources for felt earthquakes in European Russia have until recently been written documents for the historical period (Kondorskaya and Shebalin 1977; Panasenko 1980; Godzikovskaya et al. 2010a; Nikonov 2013; Tatevossian and Mäntyniemi 2014). However, different combined earthquake catalogs for the historical period occasionally reported different parameters for the same earthquakes. In addition, there are frequent misprints, gaps, and inaccurate or unreliable data (Godzikovskaya et al. 2010a; Nikonov 2013), which is a thing that is rather frequent in earthquake catalogs generally (Desherevskii and Sidorin 2014).

With regard to northern European Russia with its low level of seismicity, reliability for the earthquake parameters of individual events is important. For this reason, the problem of developing a reliable earthquake catalog for the historical period is a major challenge facing the study of the region. Several researchers have to varying degrees been involved with this scientific issue. Among these may be mentioned the names of Panasenko, G. D., Godzikovskaya, A. A., and Tatevossian, R. E. A colossal work to revise the catalog of historical earthquakes has during several decades been carried out by A.A. Nikonov, ranging between digging in primary sources and quantitative estimates of main earthquake parameters (Nikonov 2013).

The work on summarizing and correcting the evidence for earthquakes during the instrumental period, for both the entire European Russia and its component regions, with data added for the historical period, can be found in Panasenko (1980), Assinovskaya and Nikonov (1998), Assinovskaya (2004), Malovichko et al. (2007), Godzikovskaya et al. (2010b), and Nikonov (2013). Figure 2 shows a spatial distribution of the EEP earthquakes taken from Malovichko et al. (2007). It can be seen that the highest seismic activity occurred in the Fennoscandian Shield (within the Kola Peninsula and adjacent areas) and the Middle Urals.

Malovichko et al. (2007) have estimated to some approximation the lowest magnitudes of complete reporting for different phases of instrumental observation in European Russia:

Pre-instrumental period (before 1906), Mrep = 5.0;

The first phase of the instrumental period (1907–1967), Mrep = 4.5

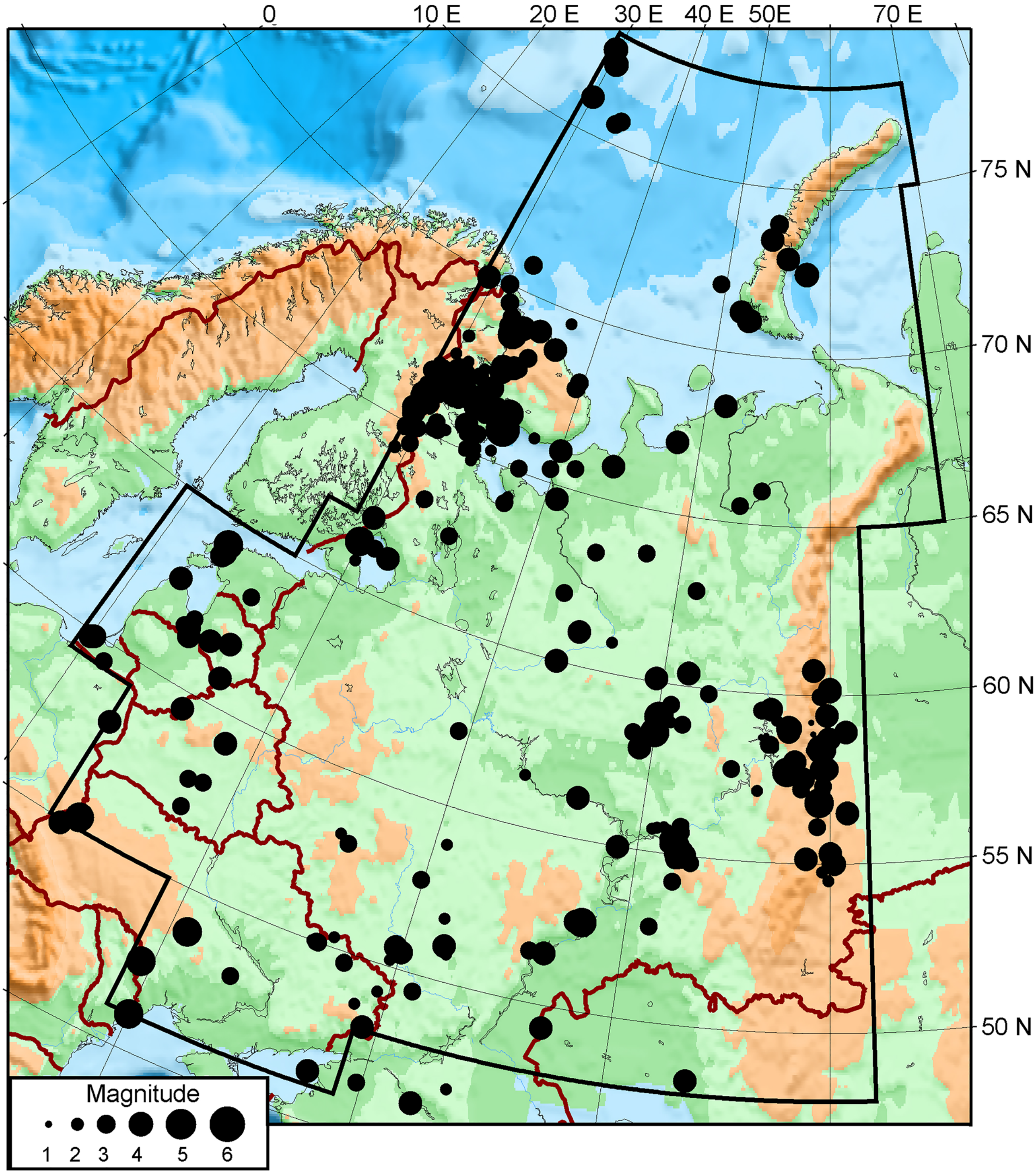

Fig. 2 A map of epicenters for the East European Platform for the period between 1467 and 2005 after Malovichko et al. (2007)

The second phase of the instrumental period (1968–1987), Mrep = 3.5–4.0

The third phase of the instrumental period (1988–2005), Mrep = 3.0–3.5

These values refer to the entire European Russia, while being occasionally lower for some individual regions. For example, the magnitudes for the northwest territory can be taken to be those in Ahjos and Uski

(1992), which were calculated for all of Fennoscandia: 4.0–4.5 since 1940; 3.5–3.9 since 1970; and no more than 2.0 since 1985.

It is to be noted that, while the naturally occurring earthquakes have comparatively low magnitudes in northern European Russia, there have been regular occurrences of man-induced seismic events at numerous and rather large industrial quarries (Adushkin 2016). Estimates of the seismic energy emitted by quarry blasts show that they are two to four orders higher than the seismic energy due to tectonic earthquakes (Adushkin 2013). For this reason, the issue of contamination in seismic catalogs with man-induced events is an urgent one for European Russia.

As of 2018, the instrumental observations in northern European Russia were carried out by the N. Laverov Federal Center for Integrated Arctic Research (network code is AH), the Kola Branch of Geophysical Survey of Russian Academy of Sciences (network code is KOGSR), the Institute of Geology of the Karelian Research Centre of the Russian Academy of Sciences, Institute of Geology of the Komi Science Center of the Ural Branch of the Russian Academy of Sciences (IG Komi SC UB RAS), the Central Branch of the Geophysical Survey of the Russian Academy of Sciences (GS RAS) (network code is OBGSR), Institute of Seismology of the University of Helsinki (Finland, network code is HE), Sodankylä Geophysical Observatory of the University of Oulu (Finland, network code is FN), the NORSAR Agency (Norway, network code is NO), and the Norwegian National Seismic Network (University of Bergen, Norway, network code is NS) (Fig. 1).

3 Description of dataset and methods

The data from the Institute of Seismology of the University of Helsinki (Finland) (network code is HE) and from the Russian regional seismic networks were used to develop a preliminary catalog of tectonic earthquakes that occurred in northern European Russia for the period between 2005 and 2017. The selected area can be seen in Fig. 1. The preliminary catalog contains earthquakes that were recorded by at least four stations. Some individual stations of the regional networks recorded many small seismic events of manmade origin, some of which make swarms (Assinovskaya et al. 2019; Vinogradov et al. 2016). However, these events were not included in the preliminary catalog because the number of stations that have recorded them are below our cutoff value for the number of stations that must record an event or else because the respective epicenters were outside our area of study.

The choice of the Institute of Seismology of the University of Helsinki catalog as one of our main data sources for our preliminary catalog was dictated by the accessibility and completeness of continually updated information coming from near stations. All the recorded events in the Institute of Seismology data base are identified by the type of source (manmade or tectonic). Each earthquake was additionally tested to see whether it was a tectonic event based on the criteria developed at the Kola Branch of GS RAS (Asming and Kremenetskaya 2002; Kremenetskaya et al. 2002; Ringdal et al. 2002). As well, we also used data from the monitoring of infrasound events conducted by workers at the Kola Branch of GS RAS based on records made by the Apatity infrasound array (Kremenetskaya et al. 1997; Asming and Kremenetskaya 2013). Four seismic events have been unambiguously identified as blasts. However, we have not succeeded in testing many seismic events because of low signal/noise ratios in seismic waveforms. We therefore do not exclude the possibility of manmade seismic events still remaining in the catalog. However, the probability of such an occurrence has been reduced to a minimum. Even if some manmade events do remain in the catalog, they must not significantly affect patterns in the distribution of recent seismicity for northern European Russia.

Each earthquake in the preliminary catalog was supplied with a summary bulletin containing arrival times of seismic phases. These bulletins were based on data coming from seismic stations in all the nine regional networks listed above. The arrival times for stations in the HE, FN, NS, and NO networks were taken from bulletins of the International Seismological Centre (ISC) and of the Institute of Seismology of the University of Helsinki. The arrival times at stations in the AH, KOGSR, and OBGSR networks and those operated by the Institutes of Geology at the Karelian Research Centre of the RAS and the IG Komi SC UB RAS were read from original seismic records using the WSG facility (Krasilov et al. 2006) by minimizing the residuals and with the help of the EL (Asming and Fedorov 2015).

The hypocenter parameters were revised by the generalized beamforming method (Kvaerna and Ringdal 1996) in a refined version, which is the NAS (New Association System) program (Asming and Prokudina

2016; Fedorov et al. 2019). The starting space-time point for the program was an approximate location of the seismic event and its approximate time of origin. The NAS revises the coordinates and time around the point. The next step was to choose a circle of large radius around the starting point (the value 250 km was used here) where a more accurate location was determined. The circle was covered by overlapping circles of shorter radii, thus making a grid. A rating function R(c,t) was calculated for each lesser circle to test the hypothesis that the event occurred in a cell c at time t. The grid was diminished several times. At each step, three fourths of the cells with the lowest ratings were eliminated, with each remaining cell being divided into four lesser ones. The ratings were revised for these diminished cells.

This search was carried out for a set of fixed depths (this study used depths between 0 and 100 km at steps of 5 km). Finally, the preliminary location of the event was chosen to be the cell having the highest rating. The time t_0 at which the rating function reached the maximum was taken to be an estimated time of origin. Only those phases which have made nonzero contributions into that maximum rating were treated as being associated with the event. This approach can automatically ignore phases having unrealistic (erroneous) onset times. This is especially important when times measured on older analog seismograms are used.

The second location phase involved minimization of occurrence time residuals to revise the location based on the times and their weights thus determined, producing a confidence region (an error ellipse), which arises instead of the true location point because the quantities that are important for location are subject to error. Calculation of a confidence region thus requires, apart from knowledge of some phases and coordinates of the sensors, also estimates of the errors in the velocity model Δv and of arrival times Δt for different wave types. In this study, we take the uncertainty the velocity model involves to be 0.15 km/s and the errors of arrival time measurement to be 0.3 s.

The relocation was based on the BARENTS travel time model (Kremenetskaya et al. 2001). The model was developed for Fennoscandia, the Baltic shield, and adjacent areas. In its upper layers, the model is a simplified average of various models developed for parts of the region. Below the Moho, the model uses the ak135 model layers (Kennett et al. 1995). Verification of the modified method and selection of the travel time model used data for four nuclear explosions that occurred in the area of the Novaya Zemlya Archipelago and in northern European Russia (Morozov et al. 2018a). This verification showed that the modified method and the BARENTS travel time model provide sufficient accuracy for event location in the region.

4 Discussion of results

A total of 139 earthquakes with magnitudes M_L between 0.1 and 4.6 have been recorded in the area of study from 2005 through 2017 (Table 1). The completeness of the catalog can be estimated from Fig. 3. All earthquakes with M_L from 1.3 upward have been recorded, but this applies, not to the entire area of study, but mostly to its northwestern part where the bulk of earthquakes have occurred.

For 80% of the earthquakes (N = 111), the major axis of the error ellipse is no longer than 10 km with fixed error parameters for the velocity model (0.15 km/s) and arrival times (0.3 s) (Fig. 3). It was only for five earthquakes that the major axis was longer than 25 km. This is a typical occurrence for the eastern part of northern European Russia and the Novaya Zemlya area, because

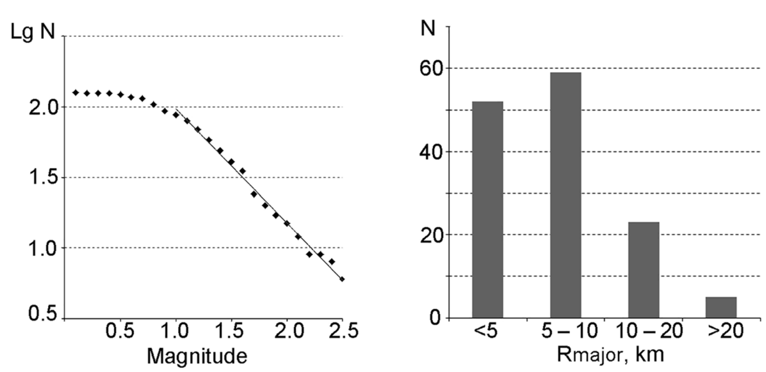

Fig. 3 A cumulative plot for the recurrence of earthquakes that occurred in northern European Russia (left) and a diagram showing the distribution of the major axis in the error ellipse, Rmajor

Table 1 Catalog of relocated seismic events in an area of the northern European Russia for the period between 2005 and 2017

No.	Date			Time			Hypocenter			Error ellipse			Calculation parameters			Magnitude				Type of source
	Year	Month	Day	Hour	Minute	Second	φ,°	λ,°	h, km	AzMajor,°	Rminor, km	Rmajor, km	Nst/Ndef	Distances*, km	Gap, °	ML (HE)	ML (KOGSR)	ML (AH)	ML (KOMI)	
1	2005	02	16	06	48	31.2	67.41	32.05	(16) 6–32	150	4.0	5.1	10/17	48–814	97	1.7				Tectonic
2	2005	03	01	20	00	07.4	69.85	33.10	0											Blast
3	2005	03	15	16	17	17.1	69.91	33.06	0											Blast
4	2005	03	18	01	49	43.7	67.14	31.91	(3) 0–17	140	5.0	8.4	6/10	70–789	121	1.1				Tectonic
5	2005	08	22	02	42	41.2	66.39	30.80	(10) 4–16	90	4.3	7.4	6/11	52–293	267	0.8				Undeterminable
6	2005	10	01	01	22	59.1	67.24	32.54	(10) 0–24	120	4.2	7.9	10/16	47–583	143	1.6				Tectonic
7	2005	10	19	03	15	44.6	66.88	31.00	(8) 0–22	90	4.6	10.7	5/8	80–195	275	1.2				Undeterminable
8	2005	10	22	17	46	44.8	64.49	40.95	(0) 0–13	70	10.4	14.5	11/22	24–1020	235	2.8		2.9		Tectonic
9	2005	10	23	00	34	06.3	66.64	33.29	(16) 0–51	100	5.6	11.8	12/21	107–639	200	1.6				Tectonic
10	2005	12	02	00	03	57.7	66.89	31.36	(15) 8–22	110	2.7	4.8	10/20	97–382	140	1.6				Tectonic
11	2005	12	12	01	46	03.8	66.87	31.02	(14) 5–22	120	2.9	5.4	10/15	84–441	133	1.2				Tectonic
12	2006	01	13	21	35	01.3	66.64	31.09	(0) 0–2	130	1.9	5.5	7/11	72–291	174	0.9				Undeterminable
13	2006	02	02	12	29	10.8	66.59	29.30	(5) 0–99	60	3.8	9.8	4/8	27–287	205	1.1				Undeterminable
14	2006	02	18	08	10	02.8	66.84	32.44	(0) 0–13	120	4.0	10.1	10/18	88–632	189	1.7				Tectonic
15	2006	03	30	10	46	02.1	70.68	52.88	(35) 0–99	110	19	40	13/19	836–1555	272	2.6				Undeterminable
16	2006	04	04	01	47	02.6	66.28	31.01	(3) 0–10	130	2.9	4.8	11/19	64–423	148	1.1				Undeterminable
17	2006	04	13	13	25	14.2	66.72	29.33	(11) 0–21	100	3.0	5.1	8/12	37–354	113	1.0				Undeterminable
18	2006	07	11	18	24	41.9	67.31	32.27	(10) 0–27	120	4.3	6.6	15/27	45–715	149	2.1				Tectonic
19	2006	07	23	01	32	08.8	66.00	39.58	(29) 2–99	60	7.3	10.9	19/33	218–1036	192	2.3				Tectonic
20	2006	10	25	12	24	42.7	66.94	31.07	(10) 0–33	130	2.6	12.9	5/7	91–144	175	0.7				Undeterminable
21	2006	12	31	05	35	56.0	65.66	32.02	(0) 0–3	60	4.2	11.2	7/10	104–313	235	0.5				Undeterminable
22	2007	03	13	14	31	28.6	66.29	31.16	(24) 18–30	130	2.9	5.5	18/30	63–549	146	1.9				Tectonic
23	2007	03	29	22	53	21.9	66.15	30.54	(0) 0–5	90	2.8	5.8	9/14	28–240	264	0.8				Undeterminable

Table 1 (continued)

No.	Date			Time			Hypocenter			Error ellipse			Calculation parameters			Magnitude				Type of source
	Year	Month	Day	Hour	Minute	Second	φ,°	λ,°	h, km	AzMajor,°	Rminor, km	Rmajor, km	Nst/Ndef	Distances*, km	Gap, °	ML (HE)	ML (KOGSR)	ML (AH)	ML (KOMI)	
24	2007	04	08	14	35	13.7	66.15	33.09	(5) 0–15	120	3.6	7.1	13/23	142–625	189	2.4				Tectonic
25	2007	08	01	04	31	57.1	66.58	31.28	(10) 2–18	130	2.1	5.1	8/16	78–226	183	1.3				Tectonic
26	2007	08	03	00	59	38.4	66.02	30.36	(18) 15–22	90	2.6	5.0	7/12	16–227	258	0.4				Undeterminable
27	2007	08	19	22	56	03.3	69.64	33.10	(33) 3–98	40	6.3	12.7	29/56	226–1377	242	3				Tectonic
28	2007	09	11	08	04	48.7	69.73	29.99	(0) 0–99	40	6.6	20.9	4/6	108–406	268	1.3				Undeterminable
29	2007	10	30	00	19	16.0	66.63	30.91	(20) 0–99	100	2.7	9.2	4/6	60–135	238	0.5				Undeterminable
30	2007	11	23	04	22	30.3	66.30	32.75	(0) 0–10	120	3.4	7.7	11/20	130–596	219	1.4				Undeterminable
31	2008	01	27	01	54	25.5	68.19	29.74	(8) 0–14	40	2.5	3.4	9/16	48–254	143	1.0				Tectonic
32	2008	01	27	03	24	23.8	68.18	29.76	(12) 0–27	30	3.0	3.9	5/9	49–228	143	1.2				Undeterminable
33	2008	05	10	15	05	08.4	66.86	31.77	(6) 0–14	110	2.9	5.5	16/28	98–531	151	1.6				Tectonic
34	2008	06	22	18	01	41.2	68.19	30.79	(16) 8–23	60	3.6	5.0	12/21	70–298	164	1.3				Tectonic
35	2008	07	12	17	17	14.8	68.39	35.78	(25) 12–52	60	7.4	10.8	14/22	135–856	227	2.7				Tectonic
36	2008	09	12	20	14	25.6	68.72	33.29	(15) 0–65	70	6.8	18.0	7/9	185–331	248	1.2				Undeterminable
37	2008	09	22	23	21	00.5	61.28	51.58	10f	30	6.2	21.0	14/26	319–1492	161				3.2	Tectonic
38	2008	10	19	23	29	10.0	66.87	29.16	(6) 0–23	70	1.4	2.7	9/18	58–146	149	0.5				Undeterminable
39	2008	10	25	03	09	45.3	66.54	32.42	(0) 0–7	120	2.9	7.2	11/20	122–422	220	1.3	1.6			Tectonic
40	2009	05	25	20	58	04.3	67.01	31.82	0											Blast
41	2009	08	31	15	17	50.8	66.31	31.05	(28) 22–33	110	3.3	6.1	16/30	62–548	183	1.5				Tectonic
42	2009	09	08	00	23	48.3	66.78	31.13	(18) 11–24	100	3.0	4.1	21/38	81–777	82	2.1				Undeterminable
43	2009	09	08	04	42	16.9	66.79	31.08	(14) 8–22	110	2.5	5.6	11/18	79–383	168	1.4				Undeterminable
44	2009	10	20	04	45	43.9	57.78	50.36	5	20	6.6	24.0	11/19	315–1430	199				3.4	Tectonic
45	2009	11	16	04	27	26.6	66.04	30.03	(7) 3–10	110	2.4	4.7	20/37	5.5–495	167	1.6				Tectonic
46	2009	11	28	14	32	23.6	66.26	33.00	(1) 0–13	100	3.6	4.6	10/16	138–315	167	1.6				Tectonic

Table 1 (continued)

No.	Date			Time			Hypocenter			Error ellipse			Calculation parameters			Magnitude				Type of source
	Year	Month	Day	Hour	Minute	Second	φ,°	λ,°	h, km	AzMajor,°	Rminor, km	Rmajor, km	Nst/ Ndef	Distances*, km	Gap, °	ML (HE)	ML (KOGSR)	ML (AH)	ML (KOMI)	
47	2009	12	03	19	55	45	66.35	31.28	(13) 7–21	100	3.5	6.1	9/16	70–236	247	0.8				Undeterminable
48	2009	12	11	23	53	52	67.08	31.80	(11) 3–18	120	2.4	4.7	11/20	78–376	171	1.2				Tectonic
49	2010	02	25	01	42	13.8	66.43	30.53	(0) 0–7	90	2.2	4.7	10/17	40–254	220	0.7				Undeterminable
50	2010	03	27	23	06	55.8	66.24	32.02	(18) 1–24	170	7.4	12.9	6/11	93–180	333	0.7				Undeterminable
51	2010	04	06	04	49	03.4	66.90	31.08	(6) 0–12	110	1.9	3.5	12/23	87–358	159	1.3				Undeterminable
52	2010	05	20	01	33	48.3	66.31	32.12	(25) 16–34	30	7.9	8.5	6/11	98–268	316	0.7				Undeterminable
53	2010	09	05	05	17	33.2	66.20	30.74	(2) 0–7	130	2.8	5.2	17/29	42–529	176	1.4				Tectonic
54	2011	01	19	17	18	14	61.57	51.16	18	40	5.2	20.4	7/14	24–711	163				2.6	Tectonic
55	2011	01	20	14	37	00.0	65.35	30.54	(10) 2–16	60	2.3	4.0	10/17	52–273	123	0.9				Undeterminable
56	2011	04	25	02	38	37	59.57	50.68	15	40	6.1	11.4	16/29	114–2490	73				3.4	Tectonic
57	2011	06	16	15	44	06.5	66.59	31.58	(0) 0–5	100	4.5	9.4	9/15	89–523	214	1.6				Undeterminable
58	2011	08	13	11	54	52.2	66.18	34.23	(0) 0–48	120	6.4	12.1	6/11	173–272	272	1.2				Tectonic
59	2011	10	11	20	04	59.4	66.45	30.68	(20) 15–25	110	3.0	4.9	14/22	47–404	138	1.2				Undeterminable
60	2011	11	15	17	48	10.2	67.43	31.73	(0) 0–4	140	2.5	3.4	11/20	58–345	131	1.5	1.9			Tectonic
61	2012	01	03	00	01	37.9	68.14	29.30	(0) 0–99	70	3.4	6.0	4/8	44–220	206	1.1				Undeterminable
62	2012	01	08	20	54	25	66.81	31.46	(0) 0–6	110	3.1	5.5	19/30	99–606	145	0.7				Undeterminable
63	2012	02	15	06	48	08.7	66.46	32.09	(4) 0–22	110	5.2	16.4	7/10	100–428	272	1.2				Undeterminable
64	2012	03	27	07	13	12.5	66.11	30.36	(8) 3–13	90	2.3	2.7	10/19	22–271	136	0.9				Undeterminable
65	2012	04	22	20	09	32.4	67.01	31.32	(6) 0–13	110	2.3	3.3	12/23	97–242	107	1.3				Undeterminable
66	2012	04	30	08	48	27.4	65.78	30.80	(0) 0–12	100	2.2	3.6	6/10	45–128	288	0.8				Undeterminable
67	2012	08	27	07	29	45.3	66.16	30.77	(12) 7–18	100	2.9	6.0	7/12	36–285	236	1				Undeterminable
68	2012	10	07	03	43	12.9	66.21	47.84	(26) 0–99	50	8.6	19.0	13/25	526–1656	170	1.6				Undeterminable
69	2012	10	11	15	00	48.0	65.82	30.35	(25) 19–30	100	1.9	3.9	5/9	27–92	262	0.5				Undeterminable

Table 1 (continued)

No.	Date			Time			Hypocenter			Error ellipse			Calculation parameters			Magnitude				Type of source
	Year	Month	Day	Hour	Minute	Second	φ,°	λ,°	h, km	AzMajor,°	Rminor, km	Rmajor, km	Nst/Ndef	Distances*, km	Gap, °	ML (HE)	ML (KOGSR)	ML (AH)	ML (KOMI)	
70	2012	12	04	07	13	09	65.89	30.15	(5) 1–8	100	2.7	5.8	11/19	19–263	217	1.1				Undeterminable
71	2012	12	24	06	22	39	66.77	64.36	11	70	7.2	9.9	76/104	343–8477	48				3.9	Tectonic
72	2013	03	28	07	02	16.5	63.97	41.50	(21) 8–36	150	6.8	8.1	31/59	82–2596	83	2.9		3.4		Tectonic
73	2013	04	03	14	49	35.0	66.99	30.19	(0) 0–6	100	2.3	3.6	16/28	74–383	128	1.5				Tectonic
74	2013	04	26	19	51	08.2	68.04	29.37	(6) 0–13	70	3.3	6.3	7/12	32–230	188	0.7				Undeterminable
75	2013	05	01	22	52	21.7	66.49	30.79	(22) 15–29	120	2.2	4.5	10/18	54–395	172	1.3				Tectonic
76	2013	11	26	20	39	07.1	66.44	30.85	(15) 11–22	80	4.0	6.9	7/12	57–217	269	0.5				Undeterminable
77	2013	11	30	22	16	20.1	65.48	31.73	(15) 0–59	20	6.2	9.1	6/8	105–656	142	0.8				Undeterminable
78	2014	01	28	04	41	38	62.36	59.54	5	60	7.1	11.0	9/18	238–1211	137				3.4	Tectonic
79	2014	02	25	18	53	06.1	66.43	32.46	(1) 0–10	120	2.6	3.7	12/21	122–431	118	1.7				Tectonic
80	2014	03	20	13	56	40.7	64.87	35.52	(41) 29–57	50	6.3	8.2	13/23	25–543	128	1.2				Undeterminable
81	2014	04	08	00	45	38.6	65.98	31.39	(0) 0–2	110	3.4	5.7	7/13	63–246	263	0.6				Undeterminable
82	2014	08	20	02	27	38.0	66.30	31.83	(4) 0–12	120	2.9	3.6	10/17	92–337	115	1.3				Tectonic
83	2014	08	29	23	37	39.2	66.60	31.56	(1) 0–8	100	3.4	8.5	7/13	88–241	263	0.9				Undeterminable
84	2014	09	05	02	27	28.3	66.44	31.70	(3) 0–10	90	3.0	4.1	9/15	92–320	121	0.8	1.2			Undeterminable
85	2014	09	08	04	15	11.7	67.96	30.17	(3) 0–11	10	2.8	3.1	6/11	33–256	138	1				Tectonic
86	2014	09	12	22	09	43.3	66.32	31.51	(26) 15–32	110	4.0	8.5	5/9	71–155	273	0.6				Undeterminable
87	2014	10	02	12	19	23.1	66.40	32.53	(0) 0–7	120	3.0	4.3	14/23	123–508	119	1.4				Tectonic
88	2014	10	11	00	32	45.6	65.94	32.43	(0) 0–4	100	5.6	10.1	6/8	114–309	243	0.9				Undeterminable
89	2014	11	23	23	20	11.6	66.50	31.53	(9) 0–21	100	3.4	6.8	6/11	86–170	251	1.1				Undeterminable
90	2014	11	30	09	43	19.9	67.15	32.53	(13) 2–25	140	3.6	6.4	8/12	57–393	178	0.7				Undeterminable
91	2014	12	13	21	10	40.1	66.28	31.18	(21) 15–27	110	3.1	4.9	11/17	62–307	164	1.2				Undeterminable
92	2015	01	04	13	58	06	64.55	60.72	14	50	5.0	6.5	157/208	430–7639	26				4.6	Tectonic

Table 1 (continued)

No.	Date			Time			Hypocenter			Error ellipse			Calculation parameters			Magnitude				Type of source
	Year	Month	Day	Hour	Minute	Second	φ,°	λ,°	h, km	AzMajor,°	Rminor, km	Rmajor, km	Nst/Ndef	Distances*, km	Gap, °	ML (HE)	ML (KOGSR)	ML (AH)	ML (KOMI)	
93	2015	01	08	06	20	41.2	66.17	29.96	(19) 16–25	90	1.9	3.3	5/8	15–95	227	0.1				Undeterminable
94	2015	02	15	03	00	35.9	65.95	30.07	(9) 0–15	100	1.3	2.8	6/10	12–88	234	0.3				Tectonic
95	2015	02	28	19	33	49.1	66.31	31.85	(0) 0–14	130	2.4	6.6	6/10	92–260	233	1.1	1.5			Tectonic
96	2015	03	20	14	46	39.0	60.31	43.83	(0) 0–23	170	7.7	16.1	19/32	175–1329	183	2.7				Tectonic
97	2015	03	21	14	14	19	62.93	58.22	12	60	6.9	11.7	17/30	226–1573	152				3.1	Tectonic
98	2015	04	02	08	16	56.6	68.31	29.17	(0) 0–7	50	3.1	4.6	8/14	65–819	126	1				Undeterminable
99	2015	04	03	18	50	12.7	69.36	30.67	0											Blast
100	2015	04	04	20	23	38.9	66.17	30.74	(5) 0–12	110	4.2	10.2	5/8	39–286	263	0.6				Undeterminable
101	2015	04	22	02	08	54.7	66.95	31.10	(0) 0–6	100	2.5	4.8	9/15	89–220	161	0.7				Tectonic
102	2015	05	10	14	03	11.7	66.74	31.13	(21) 15–25	130	2.2	3.6	14/25	80–334	82	1.4				Tectonic
103	2015	05	31	00	40	34.5	66.68	33.21	(0) 0–8	130	3.8	9.6	8/11	104–317	222	0.8				Undeterminable
104	2015	06	23	06	15	59.3	66.88	31.03	(13) 6–21	100	2.5	4.5	10/16	84–219	153	1.0				Tectonic
105	2015	06	26	03	45	48.9	66.57	32.03	(23) 13–29	120	2.7	5.2	8/13	112–264	163	0.7	1.7			Undeterminable
106	2015	06	29	13	05	09.1	65.93	31.88	(19) 14–23	110	2.5	3.0	18/31	89–512	112	1.9	2.3			Tectonic
107	2015	07	03	17	05	37.9	57.95	46.38	14	30	5.8	7.4	45/67	191–2672	50				3.8	Tectonic
108	2015	07	05	06	11	39	58.00	46.44	15	10	7.6	16.4	14/28	186–1617	181				3.5	Tectonic
109	2015	07	06	17	31	34.8	66.39	31.83	(15) 7–23	110	3.4	4.0	10/18	94–560	115	1.7	2.0			Tectonic
110	2015	07	12	11	31	57.2	66.45	31.42	(10) 5–15	100	3.0	5.8	9/17	80–237	249	0.8				Undeterminable
111	2015	08	01	04	31	04.4	66.21	30.55	(13) 8–20	90	2.0	3.8	7/12	32–178	226	0.7				Undeterminable
112	2015	09	11	19	23	52.2	66.36	31.33	(20) 16–26	110	2.4	3.0	27/50	74–868	59	2.4				Tectonic
113	2016	01	12	19	14	50.2	66.96	29.76	(14) 0–32	80	1.9	4.8	5/8	66–147	181	0.4				Undeterminable
114	2016	02	28	17	48	07.0	67.00	32.01	(16) 8–23	110	2.7	3.9	24/43	79–771	57	1.8	2.1			Tectonic
115	2016	04	03	00	04	27.0	67.52	32.09	(0) 0–6	160	3.3	4.9	7/13	40–282	152	1.0	1.5			Tectonic
116	2016	04	06	19	09	34.0	59.46	52.20	11	30	3.7	5.4	7/14	147–503	110				2.4	Tectonic

Table 1 (continued)

No.	Date			Time			Hypocenter			Error ellipse			Calculation parameters			Magnitude				Type of source
	Year	Month	Day	Hour	Minute	Second	φ,°	λ,°	h, km	AzMajor,°	Rminor, km	Rmajor, km	Nst/Ndef	Distances*, km	Gap, °	ML (HE)	ML (KOGSR)	ML (AH)	ML (KOMI)	
117	2016	04	23	00	09	24.9	67.63	33.31	(13) 3–19	170	3.9	8.4	10/15	16–493	106	1.4				Tectonic
118	2016	05	17	11	13	19.4	66.90	30.16	(1) 0–6	90	2.6	4.0	17/32	98–380	121	1.5				Tectonic
119	2016	05	26	04	46	00.7	66.04	35.66	(34) 2–99	90	5.8	12.5	10/18	197–436	242	1.1	2.0			Tectonic
120	2016	06	13	06	16	09.2	69.58	33.78	(24) 14–32	30	4.0	8.5	11/17	64–476	196	2.1				Undeterminable
121	2016	06	19	22	33	25.4	67.05	30.05	(5) 0–12	90	2.7	3.7	19/32	79–388	114	1.5				Tectonic
122	2016	06	23	01	30	33.9	59.22	42.84	5f	20	7.1	14.8	12/23	261–1406	139				3.4	Tectonic
123	2016	07	09	17	38	20.0	67.22	32.30	(10) 0–29	140	3.7	6.9	10/15	53–399	168	0.8	1.3			Tectonic
124	2016	07	30	21	42	24.5	66.45	32.94	(3) 0–13	120	3.0	5.5	17/29	113–573	167	1.5	1.9			Tectonic
125	2016	08	03	15	49	55.4	66.35	30.68	(14) 10–18	110	2.9	3.6	21/32	49–749	89	1.6				Tectonic
126	2016	08	07	19	42	11.2	66.35	31.49	(20) 10–29	130	3.8	5.1	10/15	83–726	119	1.1				Tectonic
127	2016	09	15	08	13	02.6	66.88	30.94	(23) 18–28	100	2.7	3.4	23/43	83–705	76	2				Tectonic
128	2016	11	15	19	20	23.7	65.64	30.16	(7) 1–12	80	2.5	5.6	8/12	45–236	180	0.7				Undeterminable
129	2016	11	19	20	47	20.3	66.75	32.47	(4) 0–15	120	2.7	5.3	11/18	99–404	168	1.1	1.5			Tectonic
130	2016	11	20	18	21	00.1	66.98	31.44	(20) 12–24	110	2.3	3.4	13/23	96–375	135	1.6	1.7			Tectonic
131	2016	12	22	17	11	26.5	59.71	51.52	10	40	4.0	6.4	14/23	105–691	96				2.9	Tectonic
132	2017	01	03	10	40	31.8	66.11	31.00	(10) 4–16	120	3.2	4.4	17/33	50–461	162	1.8				Tectonic
133	2017	01	08	10	28	14.4	69.19	33.81	(21) 5–45	30	4.6	5.5	11/19	51–532	162	2.0				Tectonic
134	2017	03	08	01	41	34.2	65.87	30.18	(20) 16–25	80	3.4	4.7	16/31	21–452	122	1.4				Undeterminable
135	2017	03	19	17	30	01.1	66.92	31.61	(6) 0–16	120	2.7	4.2	15/24	98–702	98	2.0				Tectonic
136	2017	03	27	00	05	17.3	66.31	30.99	(19) 12–26	100	3.5	7.0	5/9	55–219	208	1.0				Undeterminable
137	2017	05	20	08	30	00.9	66.82	31.12	(0) 0–5	90	3.0	7.7	5/10	92–223	244	1.2				Undeterminable
138	2017	05	26	21	31	34.4	66.99	31.98	(2) 0–25	110	2.9	5.4	5/9	79–180	190	0.8				Tectonic
139	2017	05	28	01	50	17.8	66.72	31.08	(9)	120	2.7	3.8	14/26	86–772	98	1.8				Tectonic

Table 1 (continued)

No.	Date			Time			Hypocenter			Error ellipse			Calculation parameters			Magnitude				Type of source
	Year	Month	Day	Hour	Minute	Second	φ,°	λ,°	h, km	AzMajor,°	Rminor, km	Rmajor, km	Nst/Ndef	Distances*, km	Gap, °	ML (HE)	ML (KOGSR)	ML (AH)	ML (KOMI)	
140	2017	06	20	20	55	55.8	61.62	49.51	4–17 3	30	4.2	6.3	5/8	63–410	112				2.1	Tectonic
141	2017	11	14	09	55	42.9	66.10	30.72	(15) 0–100	50	2.3	5.2	4/8	61–169	252	0.9				Undeterminable
142	2017	11	17	04	13	10.2	66.45	31.48	(7) 1–13	130	2.4	4.1	10/19	85–426	155	1.4				Tectonic
143	2017	12	02	15	33	51.0	67.64	33.15	(11) 7–15	160	3.0	4.5	10/19	8–339	109	1.6				Tectonic

*The range of epicentral distances (from "…" to "…")

these territories have few stations and these are far from the epicenters.

The recent seismicity in northern European Russia is observed in the form of small earthquakes. Of the 139 recorded earthquakes, only 29 had M_L above 2.0 (Table 1). The distribution of the earthquake epicenters is quite consistent with the patterns that were previously identified in Panasenko (1980), Assinovskaya (2004), Malovichko et al. (2007), Godzikovskaya et al. (2010), Nikonov (2013), and Vinogradov et al. (2016) (Fig. 4). The west of northern European Russia shows the highest seismic activity. The epicenters are confined to the Kandalaksha and Kuusamo-Kandalaksha earthquake-generating zones that were previously identified from instrumental data (Fig. 5a). The Kandalaksha zone extends northwest along the axis of the Kandalaksha Bay. The Kuusamo-Kandalaksha zone extends in the west from the major Kuusamo seismic intersection that lies in Finnish areas adjacent to Russia farther northeastward to the Kandalaksha Bay.

The occurrence of earthquakes in eastern European Russia is not unique either (Fig. 4). Earthquakes occurred repeatedly in the area both during the pre-instrumental and the instrumental period. Most epicenters in the northeastern Russian plate are confined to the Kirov–Kazhim aulacogen and to the adjacent domes of the Volga-Ural anticlise (Fig. 5b) (Udoratin and Noskova 2018). A few events occurred at the boundary between the Volga-Ural anticlise and the Mezen syneclise (Noskova and Gabsatarova 2019); these were probably caused by the tectonic stress that the edge of the Russian plate experiences in the zone of collision with the Pechora plate.

One unexpected fact is to be noted, namely, the occurrence of earthquakes in the northern Urals, within the Arctic, the Near-Arctic, and the North Urals (Fig. 4). These events can have been caused by movements on older allochthon sheets of the Urals tectonic covers. No earthquakes have been recorded there before the instrumental period and are not found in written sources during the historical period. This can in part be due to sparse population and the short written history of the region. For this reason, the recording of seismic events in the northern Urals is of special interest.

Some isolated earthquakes have been observed in different areas throughout northern European Russia for the period between 2005 and 2017 (Fig. 4). Some of these events have already been studied, as, e.g., for the southern coast of the White Sea (Morozov et al.

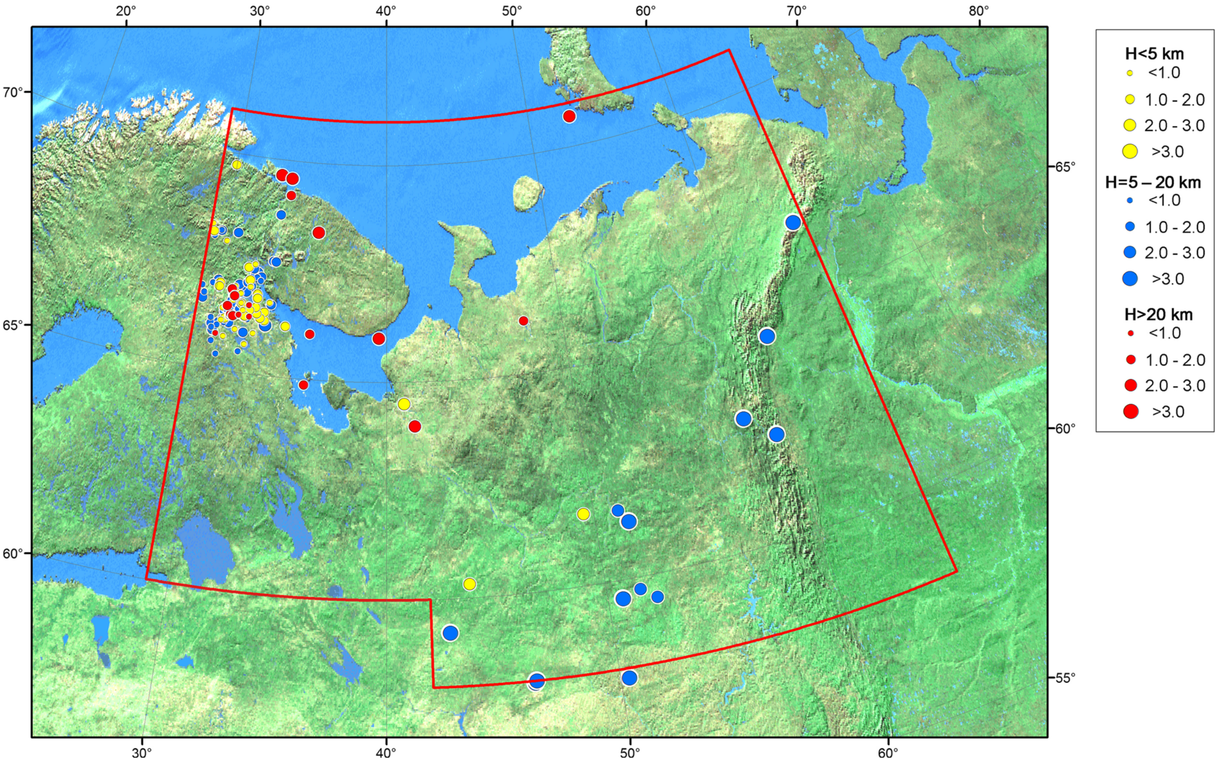

Fig. 4 A map of relocated earthquake epicenters for northern European Russia, 2005 through 2017, with magnitude and depth grades. The line encloses the area of study

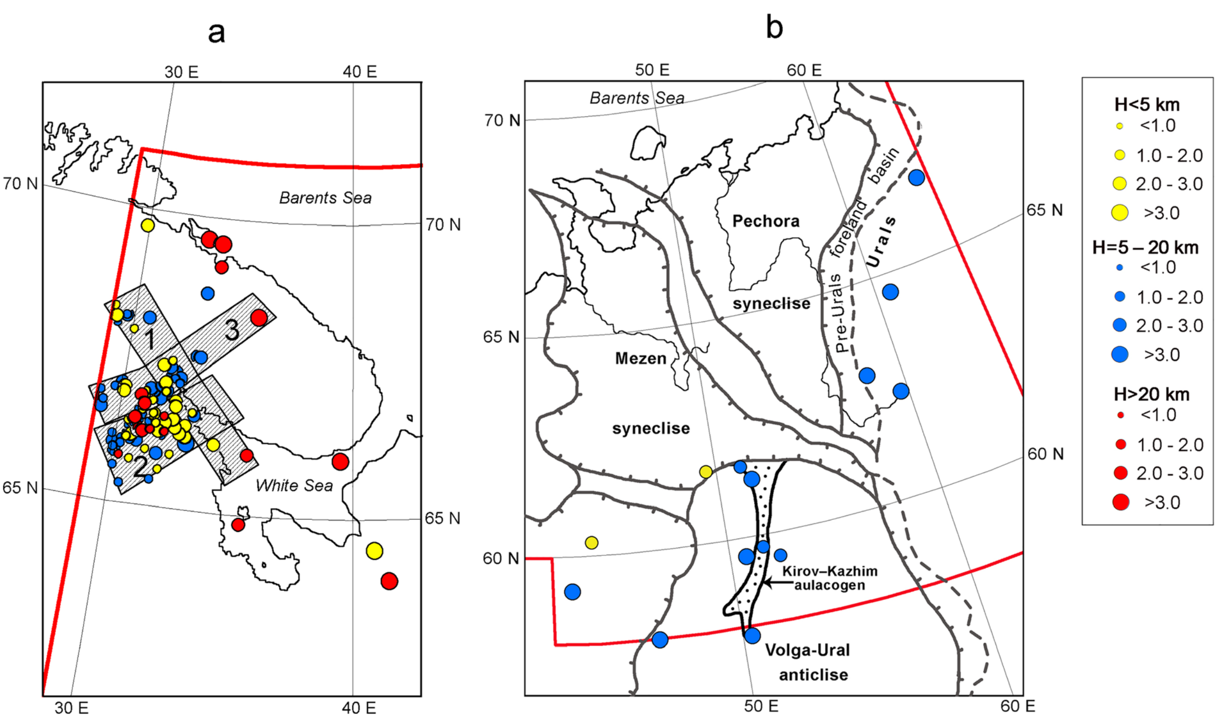

Fig. 5 Scheme of the main seismically active zones of the west of northern European Russia (**a**) and tectonic map of the northeast of the European Russia (**b**), with magnitude and depth grades: 1—Kandalaksha earthquake-generating zone; 2—Kuusamo-Kandalaksha earthquake-generating zone; 3—Khibino-Lovozeroe arthquake-generating zone. The line encloses the area of study

2018b), the northern Urals (Noskova 2016), and northeastern European Russia (Noskova and Mikhailova 2017). Other events still call for more study and clarification of the tectonic setting under which they occurred.

For each earthquake, we calculated the ranges of possible depths of focus with indication of the maximum rating function for which the epicenter parameters have been found (Table 1, Fig. 4). For some earthquakes, the ranges of possible depth are rather wide, because the absence of stations at short epicentral distances prevented a more accurate determination of the range of possible depths, even when the azimuthal coverage of the network was fairly good.

The earthquakes in northern European Russia typically occur within the crust (Fig. 4). The northwestern sector of European Russia, which shows the highest seismic activity, has its hypocenters distributed throughout the crustal depths, but the bulk of the events is in the range between 1 and 20 km. The dominant hypocentral depths are 20 km or greater in the White Sea, the Barents Sea shelf, and in the northern Kola Peninsula. The hypocenters in the east of northern European Russia and in the eastern Urals are at depths of 5 through 20 km. This is well consistent with results in Bungum and Lindholm (1997) and Assinovskaya (2004) who concluded that the earthquake-generating layer is within 5–17 km depth.

5 Conclusions

We combined catalogs, bulletins, and partly original data from the regional seismic networks and revised the hypocentral parameters of seismic events to develop a unified earthquake catalog for northern European Russia for the period between 2005 and 2017. The revision was based on the BARENTS velocity model and the same location method used (with generalized beamforming as the basis).

The resulting revised catalog was used to obtain a more accurate picture of recent seismicity in northern European Russia. Among other things, it was shown that the recent seismicity in the area of study occurs in the form of small earthquakes. The epicenter distribution is not uniform. The Fennoscandian Shield shows the highest seismic activity as estimated by seismicity rate and epicenter density. The next in seismicity level come the northeastern Russian plate and the northern Urals. All earthquakes that occurred in northern European Russia typically have their hypocenters within the crust.

The results derived in this paper set in order our notions as to how recent seismicity occurs in northern European Russia. The resulting revised catalog can serve as a basis for geological, tectonic, and geodynamic constructions, as well as providing more accurate knowledge of seismicity levels for different areas, which is a must for the area of study, because it is densely populated and has a developed industry and infrastructure.

6 Data and resources

Seismic station bulletins of the ISC are available from http://www.isc.ac.uk/ (last accessed March 2019); Seismic station bulletins of the Institute of Seismology (University of Helsinki) are available from http://www.helsinki.fi/geo/seismo/ (last accessed March 2019).

Funding information Funding research to relocated earthquakes was provided by the Russian Foundation for Basic Research (grants 19-05-00481) and by the projects no. AAAA-A17-117121270035-0 and AAAA-A18-118020290086-1. Funding research to verification of the algorithm, selection of travel time model and location error estimation was provided by the project no. 0152-2018-0028. Funding research to review the development of instrumental research was provided by the projects no. AAAA-A18-118012490072-7 and no. 0152-2018-0006.

References

Adushkin VV (2013) Blasting-induced seismicity in the European part of Russia. Izvestiya, Physics of the Solid Earth *49*(2): 258–277

Adushkin VV (2016) Tectonic earthquakes of anthropogenic origin. Izvestiya, Physics of the Solid Earth *52*(2):173–194

Ahjos T, Uski M (1992) Earthquakes in northern Europe in 1375–1989. Tectonophysics *207*(1-2):1–23

Asming VE, Fedorov AV (2015) Possibility of using a single three-component station automatic detector–locator for detailed seismological observations. Seismic Instruments *51*(3): 201–208

Asming VE, Kremenetskaya EO (2002) Study of applicability of P/S ratio criterion for discrimination of regional earthquakes and explosions in North-Western area, observed characteristics of regional seismic phases and implications for P/S discrimination in the European Arctic. Pure Appl Geophys *159*(4):721

Asming, V., & Kremenetskaya, E. (2013). Infrasound research at Kola Regional Seismological Centre, Russia In *EGU General Assembly Conference Abstracts* (Vol. 15).

Asming, V.E., Fedorov, A.V., Vinogradov, A.N., Vinogradov, Yu.A., Goryunov, V.A., Evtyugina, Z.A. (2016) Automatic system for seismic monitoring of Northwest Russia and the western sector of the Arctic. *Proceedings of the XI International Seismological* Workshop. Kyrgyzstan, 34–37. (in Russian)

Assinovskaya B.A. (2004) Instrumental data on earthquakes in the region In: *Deep structure and seismicity of the Karelian region and its margins. Ed. NV Sharov. Petrozavodsk: KarRC of RAS.*, 213-229. (in Russian)

Assinovskaya BA, Nikonov AA (1998) Felt earthquakes of the XXth century in the Eastern Baltic shield. Proc XXVI General Assembly of the Europe Seismological Commission:23–28

Assinovskaya BA, Gabsatarova IP, Panas NM, Uski M (2019) 2014-2016 seismic events around the Karelian Isthmus and their nature. Seismic Instruments 55(1)

Bungum H, Lindholm C (1997) Seismo-and neotectonics in Finnmark, Kola and the southern Barents Sea, part 2: seismological analysis and seismotectonics. Tectonophysics *270*(1-2):15–28

Collis C, Dodds K (2008) Assault on the unknown: the historical and political geographies of the International Geophysical Year (1957-8). J Hist Geogr *34*(4):555–573

Desherevskii AV, Sidorin AY (2014) Technical problems and errors in earthquake catalog studies. Sci Technol Dev 93(4): 32–41 (in Russian)

Fedorov AV, Asming VE, Jevtjugina ZA, Prokudina AV (2019) The system of automatic monitoring of the seismicity of the European Arctic. Seismic Instruments 55(1)

Godzikovskaya AA, Sergeyeva NA, Zabarinskaya LP (2010a) Regional earthquake catalogues of Russia. Seismic Instruments 46(1):86–99

Godzikovskaya, A.A., Asming, V.E., and Vinogradov, Yu.A. (2010b) *Retrospektivnyi analiz pervichnykh materialov o seismicheskikh sobytiyakh, zaregistrirovannykh na Kol'skom poluostrove i prilegayushchikh territoriyakh v XX veke* (Retrospective analysis of primary data about seismic events recorded in the Lopa Peninsula and neighboring territories in XX century), Vinogradov, A.N, Ed., Moscow: Vashpoligraficheskii partner, 141 p. (in Russian).

Kennett BLN, Engdahl ER, Buland R (1995) Constraints on seismic velocities in the Earth from traveltimes. Geophys J Int 122(1):108–124

Kondorskaya, N. V., & Shebalin, N. V. (1977). New catalog of strong earthquakes in the territory of the USSR from ancient times to 1975. *Academy of Sciences, Moscow (English translation, updated through 1977, available as Report SE-31, World Data Center A for Solid Earth Geophysics, Boulder, CO, 606 pp.).*

Krasilov SA, Kolomiets MV, Akimov AP (2006) Organization of the processing of digital seismic data with the use of WSG program complex, in Sovremennye metody obrabotki i interpretatsii seismologicheskikh dannykh (Modern Methods for Processing and Interpretation of Seismological Data). Obninsk, GS RAN, pp 77–83 (in Russian)

Kremenetskaya EO, Kuzmin IA, Raspopov OM, Kulichkov SN (1997) Seismo-acoustical equipment complex in Murmansk region. Infrasound workshop for CTBT monitoring, Santa Fe, New Mexico, Abstract, In

Kremenetskaya E, Asming V, Ringdal F (2001) Seismic location calibration of the European Arctic. Pure Appl Geophys 158(1):117–128

Kremenetskaya E, Asming V, Jevtjugina Z, Ringdal F (2002) Study of Regional surface waves and frequency-dependent Ms:mb discrimination in the European Arctic, In *Monitoring the Comprehensive Nuclear-Test-Ban Treaty: Seismic Event Discrimination and Identification* (pp. 721-733). Birkhäuser, Basel

Kvaerna T, Ringdal F (1996) Generalized beamforming, phase association and threshold monitoring using a global seismic network, In *Monitoring a Comprehensive Test Ban Treaty* (pp. 447-466). Springer, Dordrecht

Malovichko AA, Gabsatarova IP, Chepkunas LS, Starovoit OE (2007) Earthquakes and microseismicity in modern geodynamics problems of the East European Platform. Part *1*:14–66 (in Russia)

Morozov AN, Vaganova NV, Asming VE, Konechnaya YV, Evtyugina ZA (2018a) The instrumental seismicity of the Barents and Kara sea region: relocated event catalog from early twentieth century to 1989. J Seismol 22(5):1171–1209

Morozov AN, Vaganova NV, Asming VE, Mikhailova YA (2018b) Seismicity of the north of the Russian plate: relocation of recent earthquakes. Izvestiya, Physics of the Solid Earth 54(2):292–309

Nikonov AA (2013) A new stage in understanding seismicity of the East European Platform and its margins. Dokl Earth Sci 450(2):638–642

Noskova, N. N. (2016) New data on northern Urals seismicity. Vestnik IG Komi UB RAS, 3, 3-12. DOI: 10.19110/2221-1381-2016-3-3-12

Noskova, N. N., Gabsatarova, I. P. (2019) Earthquake on October 18, 2018 within the Mezen syneclise, Proceedings of the 17th Geological Congress of Komi Republic: Geology and Mineral Resources of the European Northeast of Russia, Syktyvkar: IG Komi SC UB RAS, 2, 66–69 (in Russian).

Noskova NN, Mikhailova RS (2017) The. Republic of Komi and the Kirov region, earthquakes in Northern Eurasia 20(2011): 228–238

Panasenko GD (1980) Seismicity of the eastern part of the Baltic Shield. Seismichnost'i sovremennye dvizheniya zemnoi kory vostochnoi chasti Baltiiskogo shchita:7–23 (in Russian)

Ringdal F, Kremenetskaya E, Asming V (2002) Observed characteristics of regional seismic phases and implications for P/S discrimination in the European Arctic, In *Monitoring the Comprehensive Nuclear-Test-Ban Treaty: Seismic Event Discrimination and Identification* (pp. 701-719). Birkhäuser, Basel

Shchukin, Yu. K., (2007) Dynamic geology: a basis of the system for monitoring the natural processes, in *Zemletryaseniya i mikroseismichnost' v zadachakh sovremennoi geodinamiki Vostochno-Evropeiskoi platformy* (The earthquakes and microseismicity in the problems of recent geodynamics of the East European Platform), Sharov, N.V., Malovichko, A.A., and Shchukin, Yu.K., Eds., vol. 1: *Earthquakes*, Petrozavodsk: Karelskii nauchnyi tsentr RAN, 117–172. (in Russia)

Starovoit OE (2005) Seismic observations in Russia. Zemlya Vselennaya 2:82–89 (in Russia)

Tatevossian RE, Mäntyniemi P (2014) Earthquake scenarios: a practical way to handle alternative solutions to historical earthquakes and to increase the transparency of seismic hazard assessment. Nat Hazards 72(2):549–564

Udoratin VV, Noskova NN (2018) Deep structure and seismicity of the Kirov-Kazhimsky aulacogen. IG Komi SC UB RAS, Syktyvkar 208 p. (in Russian)

Vinogradov YA, Asming VE, Kremenetskaya EO, Zhirov DV (2016) Modern seismicity in mining areas in the Murmansk Region. J Min Sci *52*(1):46–52

Yudakhin FN, Shchukin YK, Makarov VI (2003) Deep structure and recent geodynamic processes in lithosphere of the East-European Platform. Ural Branch RAS, Ekaterinburg 299 p (in Russian)